

Self-organized hyperuniformity in a minimal model of population dynamics

Tal Agranov,^{1,2} Natan Wiegenfeld,³ Omer Karin,⁴ and Benjamin D. Simons^{1,2,5}

¹*Department of Applied Mathematics and Theoretical Physics,
Centre for Mathematical Sciences, University of Cambridge, Cambridge CB3 0WA, UK*

²*Gurdon Institute, University of Cambridge, Cambridge CB2 1QN, UK*

³*Cavendish Laboratory, University of Cambridge, Cambridge CB3 0US, UK*

⁴*Department of Mathematics, Imperial College London, London, SW7 2AZ, UK*

⁵*Cambridge Stem Cell Institute, Jeffrey Cheah Biomedical Centre,
University of Cambridge, Cambridge CB2 0AW, UK*

We identify a novel scenario for hyperuniformity in a generic model of population dynamics that has been recently introduced to account for biological memory in the immune system and epigenetic inheritance. In this model, individuals' competition over a shared resource guides the population towards a critical steady state with prolonged individual life time. Here we uncover that the spatially extended model is characterized by hyperuniform density fluctuations. A hydrodynamic theory is derived by explicit coarse-graining, which shows good agreement with numerical simulations. Unlike previous models for non-equilibrium hyperuniform states, our model does not exhibit conservation laws, even when approaching criticality. Instead, we trace the emergence of hyperuniformity to the divergence of timescales close to criticality. These findings can have applications in engineering, cellular population dynamics and ecology.

Introduction – Over the last two decades, hyperuniformity has been drawing increasing attention across multiple disciplinary fields [1–3]. It describes the remarkable property in which a system of particles is statistically disordered on short length scales, yet has vanishing density fluctuations at large scales, as typically found in zero-temperature crystals [2]. Formally, the variance of the number of particles $N(\ell)$ in a given domain of size ℓ scales sub-extensively with volume, defying generic central limit theorem arguments. Mathematically, this translates to the condition

$$\frac{\text{Var}[N(\ell)]}{\langle N(\ell) \rangle} \sim \ell^{-\alpha}, \quad (1)$$

with the exponent $0 < \alpha \leq 1$ characterizing the degree of hyperuniformity [2]. Equivalently, this relation can be reformulated in terms of the vanishing of the structure factor $\lim_{q \rightarrow 0} S(q) = \lim_{\ell \rightarrow \infty} \text{Var}[N(\ell)] / \langle N(\ell) \rangle \stackrel{!}{=} 0$ [1] with

$$S(q) \equiv \frac{\langle \delta\rho(\mathbf{q}) \delta\rho(-\mathbf{q}) \rangle}{\langle \rho \rangle} \quad (2)$$

where $\delta\rho(\mathbf{q})$ represent density fluctuations around the mean density $\langle \rho \rangle$ at Fourier wave mode \mathbf{q} [4] and the S is a function of $q = |\mathbf{q}|$ from isotropy. Realizations of hyperuniformity have been established in several synthetic settings, including a-thermally jammed hard spheres [5], periodically driven emulsions [6, 7], and active Quincke rollers [8]. More recently, biologically occurring instances of hyperuniformity have been identified, including the distribution of avian photo-receptors [9, 10], the leaf vein network [11], and vegetation coverage in semi-arid landscapes [12, 13]. In a solid state setting, interest in hyperuniformity draws from their remarkable material properties, such as complete photonic band gaps [14, 15] and

optical transparency [16]. In biological contexts, hyperuniformity serves important functions such as providing uniform coverage of cell types [9, 10] or the optimization of resource-acquisition [12, 13] and resource-distribution [11].

Finding generic mechanisms that give rise to hyperuniformity remains an outstanding challenge which, if met, can unlock the potential for novel functional materials and advance our understanding of the mechanisms driving hyperuniformity in biological systems. While equilibrium dynamics with short-range interactions cannot result in hyperuniformity [17], non-equilibrium systems, such as the examples listed above, can relax to a hyperuniform state [3]. Prominent models that capture such non-equilibrium hyperuniformity include those with an absorbing state phase transition at criticality [18–21], active and passive phase separating systems during spinodal decomposition [22], and various active fluid models [8, 23, 24]. In these contexts, steady state hyperuniformity emerges when a control parameter is fine-tuned to a critical value for a phase transition. A unifying feature that underlies hyperuniformity in these systems is the effective emergence of center-of-mass conservation at criticality [18, 20, 22, 24–28]. This is manifested by a ‘superconservative’ noise whose amplitude vanishes with wave number as q^2 , leading to vanishing density fluctuations at large scales.

Here we ask whether other classes of systems can generate hyperuniformity. Specifically we focus on mechanisms that can produce hyperuniformity in a biologically realistic setting, without requiring center of mass conservation or parameter fine-tuning. To this end, we introduce a population dynamics model, motivated by programmed cell death [29–31], and formulated under general assumptions applicable to a broad class of sys-

tems. In this model, (i) agents enter through a stochastic birth-type process, while (ii) death occurs when the internal state of the agent transitions away the 'viable' regime. Finally, (iii), the viable regime is stabilized by a shared diffusive resource, analogous to survival factors consumed by cells in a tissue. This resource, depleted by the agents, acts as the control parameter of the bifurcation that stabilizes the viable state.

Together, these three ingredients define a negative feedback loop that guides the system towards a steady state where the birth rate of agents is matched by their removal (death) rate, and resource production matches its total consumption set by the population size. Remarkably, at low individual consumption rates (or high resource production rates), the steady state resource level asymptotes towards a critical threshold at the verge of the stabilization of the viable regime [32]. Mathematically, this model is a spatial extension of a zero-dimensional framework used recently to study biological memory in the context of long-term gene silencing [31], the adaptive immune system [32], and cell cycle control [33]. Unlike the classical paradigm of Self-Organized Criticality [34, 35], here the dynamics do not exhibit the hallmark feature of large-scale avalanches. On the contrary, the system displays a regular behaviour over hydrodynamics scales, allowing for systematic coarse-graining.

We find that within our dynamical framework, the population stabilizes into a steady-state where spatial correlations become hyperuniform without center-of-mass or total mass conservation, and without the fine-tuning of control parameters. Employing exact coarse-graining of an explicit dynamical model, we arrive at a time-delayed fluctuating hydrodynamics with a non-conservative noise. We trace hyperuniformity to the system's critical tuning via feedback: Over large scales, the collective response of the system to noisy individual arrivals is much quicker than the prolonged individuals' lifetime. The latter sets the timescale for density fluctuations to build up. This rapid collective response prevents the emergence of population fluctuations over large scales, resulting in hyperuniformity.

Resource competition model – Immobile agents (labeled $i = 1, 2, \dots$) are introduced stochastically in d -dimensional space at random positions \mathbf{x}_i at a mean rate per unit space volume λ . Within our minimalist modeling agents are immobile, yet endowing them with finite diffusivity will not alter our findings qualitatively [4]. An individual's lifetime τ_i is set by local environmental conditions. Generally, the dynamics which sets an agent's lifespan may be governed by a high-dimensional dynamical system. Yet in many settings, it accommodates a critical transition between finite and diverging lifespan, allowing for a major simplification in terms of detail-insensitive universal description. In the language of dynamical systems modeling, such a transition corresponds to the elimination of a stable fixed point from some effective

(possibly very high-dimensional) state space, i.e., a saddle node (SN) bifurcation. Importantly, in the vicinity of the bifurcation, the dynamics is governed by progression along a one-dimensional center manifold [36, 37], parameterized by an effective 'viability' coordinate $\nu_i(t)$, which follows the SN normal form dynamics [38]

$$\dot{\nu}_i = \nu_i^2 + \mu_i \quad (3)$$

Here, $\mu_i = \mu(\mathbf{x}_i, t)$ serves as the bifurcation control parameter. At fixed negative $\mu < 0$, the dynamics (3) supports a stable fixed point at $\nu = -\sqrt{|\mu|}$, where the agent remains 'viable'. For $\mu > 0$, the fixed point is eliminated with ν monotonically increasing towards the positive half line $\nu > 0$, leading to removal. The precise value of the viability at which new arrivals are initiated, set here to $\nu_0 < 0$, will not affect the behavior of the system [4]. The same is true for the viability threshold for 'death' set here to $\nu = 0$. In practice, small random fluctuations, not included here, would enable noisy escape from this fixed point, leading to a finite lifetime even at $\mu < 0$. While such weak fluctuations have a dramatic effect on the lifetime distribution [31], they have a sub-leading effect on density fluctuations that are at focus here [4]. Omitting them allows analytical tractability, as we discuss in the following. The dynamics (3) is then coupled to a resource field $c(\mathbf{x}, t)$, which below a threshold value c_{crit} sets the SN bifurcation. Close to the bifurcation it is enough to consider a simple linear coupling

$$\mu_i(\mathbf{x}, t) = c_{\text{crit}} - c(\mathbf{x}_i, t) \quad (4)$$

describing the elimination of the fixed point at $c < c_{\text{crit}}$. The resource is locally consumed by viable individuals, which is balanced by a fixed production rate, and is dispersed diffusively as captured by the reaction-diffusion equation

$$\dot{c} = p \left(1 - \frac{c\rho}{k} \right) + D\nabla^2 c \quad (5)$$

where p and k encode production and (inverse) consumption rates, and D is the diffusion coefficient. The number density field of surviving agents is given by

$$\rho(\mathbf{x}, t) = \sum_i \Theta(-\nu_i) \delta^d(\mathbf{x} - \mathbf{x}_i) \quad (6)$$

where the Heaviside theta-function $\Theta(\dots)$ selects for viable states, and the d -dimensional Dirac delta-function $\delta^d(\dots)$ ensures that the consumption of resource is purely local. The coupled dynamics (3-6) describe a negative feedback, which relaxes the system towards a dynamic steady state: When resource levels are elevated above the threshold level $c > c_{\text{crit}}$, new agents steadily accumulate, which, according to (5), result in increased consumption and the down-regulation of resource levels. As the individual rate of consumption is reduced

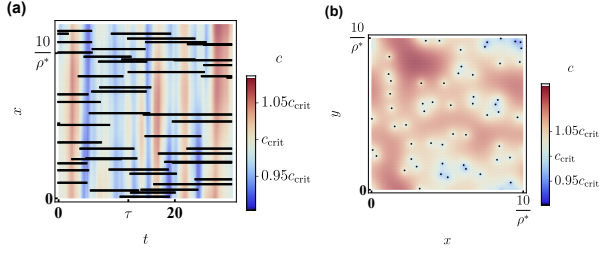


FIG. 1. Population dynamics model (3-6). (a) In a one-dimensional system. Kymograph showing the worldlines of the particles in black, and the resource field c in a color map displaying small fluctuations around the critical value $c_{\text{crit}} = 1$. (b) In a two-dimensional system. In the snapshot, particles are marked in black dots. In both panels $\mu^* \simeq 0.05$ (9).

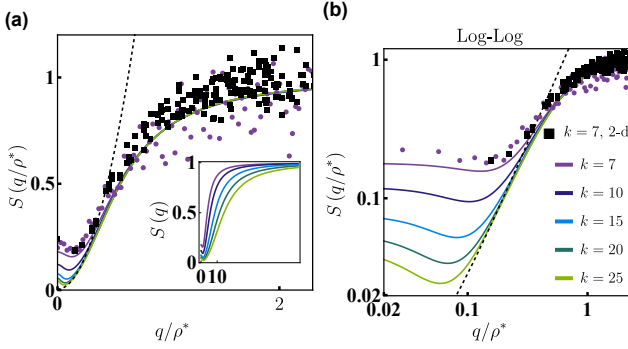


FIG. 2. Structure factor at increasing values of k approaching criticality. Solid lines are the theoretical prediction (15), while points and squares are results of numerical simulations of the dynamics (3-6) in 1-d and 2-d respectively. Dashed black line is the small q asymptotics (12) with $k = 25$.

$k^{-1} \rightarrow 0$, the system evolves towards a critical steady-state with $c \simeq c_{\text{crit}}$, as depicted in Fig. 1. As argued in the following, the particular choice of coupling to the resource (4-5) also captures the generic case, where the minimal system of Eqs. (3-6) provides a universal description of critical tuning via resource competition.

A corresponding ‘mean-field’ type analysis can be found in [31], and is briefly recapped in the following. Remarkably, going beyond a mean-field description here, we find that this dynamical steady state has hyperuniform density fluctuations as presented in Figs. 2 and 3.

Steady state at level of mean-field – At the dynamic steady state, resource production matches consumption, and the agent arrival rate matches their average removal rate. At the level of mean-field, when the steady-state density fields $\rho = \rho^*$ and $c = c^*$ are spatially homogeneous, these requirements are given, respectively, by

$$\rho^* = \frac{k}{c^*}, \quad \lambda = \frac{\rho^*}{\tau(\mu^*)} \quad (7)$$

where λ is the average arrival rate of new agents and $\tau(\mu^*)$ is the mean lifetime of agents at a fixed resource

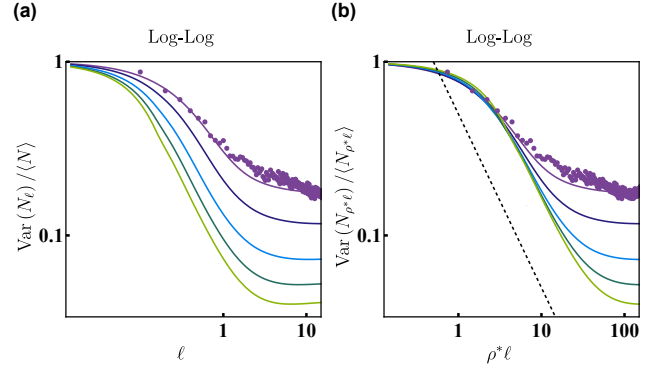


FIG. 3. Re-scaled number variance (1) color coded as in Fig. 2.

level c^* . The latter can be evaluated from Eq. (3) as

$$\tau(\mu^*) = \frac{\arctan(|\nu_0|/\sqrt{\mu^*})}{\sqrt{\mu^*}} \simeq \frac{\pi}{2\sqrt{\mu^*}} \quad (8)$$

with $\mu^* = c_{\text{crit}} - c^*$, and where we have expanded close to criticality at small μ^* . The first equality in (7) comes from (5), while the second equality is simply a manifestation of Little’s law in queueing theory [39]. Combining Eqs. (7) and (8) provides the mean value of the control parameter to leading order at small μ^*

$$\mu^* \simeq \left(\frac{\pi \lambda c_{\text{crit}}}{2k} \right)^2. \quad (9)$$

This expression shows that the critical regime can be approached either by decreasing the average arrival rate of agents λ , or decreasing the rate of consumption k^{-1} . In this work, we will explore the latter limit where, as we explain in the following, the mean-field analysis becomes exact in any space dimension, and explicit coarse-graining of the model becomes available.

We are now in a position to evaluate the generality of our model (3-6). The steady state (8) is expected to be quite general: Little’s law holds at steady state, regardless of the particular choice for dynamics; the mean density ρ^* would increase inversely with particle consumption rate for a generic resource consumption coupling. Put together, criticality $\tau \rightarrow \infty$ would be approached at small k for a general resource consumption dynamics. Lastly, hyperuniformity is found here to be insensitive to non-linearities in (4-5), making our minimal model representative of generic self-organised hyperuniformity via resource competition.

Fluctuating hydrodynamics beyond mean-field – To analyze the hyperuniform behavior quantitatively, we turn to a coarse-grained description. This hydrodynamic limit depends crucially on the emergence of the diffusive length scale $\ell_D \equiv Dk/p$ prescribed by the reaction-diffusion dynamics, Eq. (5). It represents the length scale over which the resource field c varies in the presence of the δ -function like consumption “sinks” of the agents, Eq. (6).

The hydrodynamic description emerges when this length scale is much larger than the average spacing between agents, $\ell_D \gg \ell \equiv \rho^{*-1}$, and the density field (6) becomes smoothly varying over these scales. From Eq. (7), this condition is met when $Dk^2/\rho c_{\text{crit}} \gg 1$, a limit that holds in our regime of interest, where k is sufficiently large to drive critical tuning, keeping all other parameters fixed. In this regime, nearby agents experience similar resource levels, and will have similar lifetimes, allowing for their averaging over the hydrodynamic scale. Furthermore, the noisy arrival rate of agents onto these large hydrodynamic compartments becomes deterministic with weak Gaussian white-noise corrections [40]. These two properties allows us to write down a local and time-dependent balance equation for the density of agents, akin to Little's law, that serves as a starting point for our coarse-graining procedure [4]. Moreover, under weak noise, it is sufficient to consider linearized hydrodynamics for small deviations of the fields $\delta\rho = \rho(\mathbf{x}, t) - \rho^*$ and $\delta c = c(\mathbf{x}, t) - c^*$ around their mean-field values (7). A non-trivial step in the derivation is to evaluate the agent's lifetime under time-varying resource levels. Crucially, this brings about a history dependence, which spans the agent's lifetime (8), resulting in a system of *delayed* partial differential equations

$$\delta\dot{c} = -\frac{p}{c^*}\delta c - \frac{p}{\rho^*}\delta\rho + D\nabla^2\delta c \quad (10)$$

$$\begin{aligned} \delta\dot{\rho} = & \frac{\lambda}{\mu^*} \left[\delta c - \sqrt{\mu^*} \int_0^{\tau(\mu^*)} dt' \delta c(\mathbf{x}, t-t') \sin(2\sqrt{\mu^*}t') \right] \\ & + \sqrt{\lambda} [\xi(\mathbf{x}, t) - \xi(\mathbf{x}, t-\tau(\mu^*))] \end{aligned} \quad (11)$$

with the unit variance Gaussian white-noise $\langle \xi(\mathbf{x}, t) \xi(\mathbf{x}', t') \rangle = \delta^d(\mathbf{x} - \mathbf{x}') \delta(t - t')$.

Analyzing hyperuniformity – Although the hydrodynamic equations (10-11) are time non-local, they are linear, and can be integrated to yield a closed form integral expression for the density two-point function [4]. Numerical integration of these equations shows good agreement with the results of stochastic simulation of the origin model, as shown in Fig. 2 and 3. A data collapse is observed upon rescaling length scales by individuals' spacing $q' = q/\rho^*$ and $\ell' = \ell\rho^*$. At large lengthscales, the structure factor scales as

$$S(q) \simeq \frac{\pi^2}{4} \frac{D\lambda^2}{p} q'^2 + \frac{\mu^*}{c^*}, \quad (12)$$

signaling the onset of type I hyperuniformity upon approaching criticality for any space dimension [2], see Fig. 2. This type I hyperuniformity has an exponent $\alpha = 1$ (1), see Fig. 3.

To gain insight into the origin of hyperuniformity, we first consider the case where feedback is eliminated by holding the resource field fixed at some arbitrary value $c^* < c_{\text{crit}}$. In this case, it is straightforward to show

that the dynamics maps *precisely* to a Poisson point process, with mean density $\langle \rho \rangle = \lambda\tau(\mu^*)$ [4]. Note that, consistent with the hydrodynamics, this analysis applies even when the resource is held fixed at some spatially non-uniform profile $c^*(\mathbf{x})$, resulting in an inhomogeneous Poisson point process. Such a 'maximally random' process is non-hyperuniform, with the normalized variance (1) equal to unity, $\text{Var}(N)/\langle N \rangle = 1$, for all values of ℓ . Indeed, integrating the density equation (11) with $\delta c = 0$ and vanishing initial conditions at $t = 0$ we find [41]

$$\delta\rho(\mathbf{x}, t) = \sqrt{\lambda} \int_0^{\text{Min}[t, \tau(\mu^*)]} \xi(\mathbf{x}, t-t') dt' \quad (13)$$

with the uncorrelated variance $\langle \delta\rho(\mathbf{x}, t) \delta\rho(\mathbf{x}', t) \rangle = \langle \rho \rangle \delta^d(\mathbf{x} - \mathbf{x}') \text{Min}[t/\tau, 1]$, coinciding with that of a Poisson process as soon as $t > \tau$. It is important to note that although this holds at any value of the resource, close to criticality $c^* \sim c_{\text{crit}}$, it takes a divergently long time $\tau \sim 1/\sqrt{c_{\text{crit}} - c^*}$ for fluctuations to build up and saturate the Poisson statistics. In the following, we adopt a space-time Fourier transform, where this prolonged delay can be expressed as $\langle \delta\rho(\mathbf{q}, t) \delta\rho(-\mathbf{q}, t) \rangle = \langle \rho \rangle \int d\omega \tau |\zeta(\omega\tau)|^2$ with the Fourier-transformed noise amplitude

$$|\zeta(\omega\tau)|^2 = \frac{1}{2\pi} \text{sinc}^2\left(\frac{\omega\tau}{2}\right) \quad (14)$$

and $\text{sinc}(x) = \sin(x)/x$ denotes the sinc function. Equation (14) always integrates to unity; but at large τ , it is dominated by low frequencies. Solving the hydrodynamics (10-11) in the presence of non-zero feedback, the two-point function is given by the product of the noise amplitude (14), and a non-trivial response function

$$S(q) = \int d\omega \tau |\zeta(\omega\tau)|^2 |R(q, \omega)|^2 \quad (15)$$

given by

$$|R|^2 = \frac{\omega^2 (\omega^2 + \omega_\gamma^2)}{\left[\omega^2 - \omega_0^2 \frac{\sin^2(\frac{\omega\tau}{2}) - \frac{\omega^2 \tau^2}{\pi^2}}{1 - \frac{\omega^2 \tau^2}{\pi^2}} \right]^2 + \left[\omega \omega_\gamma + \frac{\omega_0^2}{2} \frac{\sin \omega\tau}{1 - \frac{\omega^2 \tau^2}{\pi^2}} \right]^2}. \quad (16)$$

Here

$$\omega_\gamma = \frac{p}{c^*} + Dq^2, \quad \omega_0 = \sqrt{\frac{2p}{\pi}} \mu^{*-1/4} \quad (17)$$

play, respectively, a role reminiscent of damping and natural frequencies [4] and $q = |\mathbf{q}|$, from isotropy. This result is space-dimension independent, as verified in Fig. 2. Over sufficiently large scales $q \ll \rho^* \mu^{*3/4}$, the system is under-damped $\omega_\gamma \ll \omega_0$ with response peaked at the resonant frequency $\sim \omega_0$ (17), which diverges away from the typical frequency where noise is injected $\omega \sim \tau^{-1}$ (14), see Fig. 4 (a). This divergent frequency disparity leads to

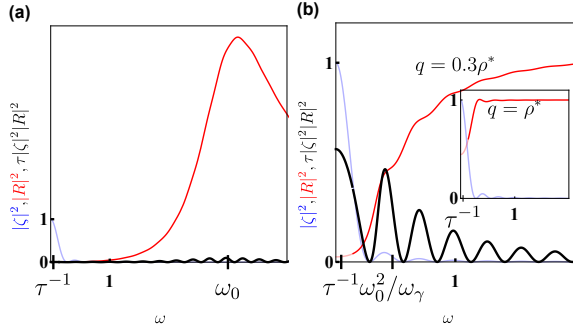


FIG. 4. The noise-response product (15). (a) At diverging scales, the system is underdamped, with the response peaked at the resonant frequency ω_0 with vanishing overlap over the noise at low $\omega \sim \tau^{-1}$. (b) Going to small, and smaller (inset) scales, the response attains a finite overlap with the noise. In all figures $\mu^* = 0.005$.

a vanishing overlap between the response $|R|^2$ and the noise $|\zeta|^2$, see Fig. 4 (a), resulting in hyperuniformity. Physically, the system responds much quicker than individual agents' lifetimes. This originates from the increased sensitivity of the particle density ρ to variations in the value of the resource close to criticality (viz. prefactor in the first line of (11)), leading to the blow up of the resonant frequency ω_0 .

This is not the case for short scales $q \sim \rho^*$, where $\omega_\gamma \gg \omega_0$. In this strongly overdamped regime, the system attains a finite response at low frequencies, see Fig. 4 (b). Ultimately, at $q \gg \rho^*$ the response approaches $|R|^2 \rightarrow 1$ uniformly (Fig. 4 inset), leading to $S \rightarrow 1$ (see Fig. 2). Indeed, the diffusion term in (10) strongly damps short-wavelength modes $\delta c(\mathbf{q}) \simeq 0$, and eliminates the feedback, reproducing the maximally disordered Poisson-like statistics at short scales. The picture is that diffusion becomes effective at short scales and prolongs the response of the particles' density. The particle-dense regions locally deplete the resource, leading to a strong incoming resource flux (the resource and particle density fields are anti-phased in space). This helps alleviate local resource depletion, delaying the response of particle density.

To evaluate the hyperuniformity exponent, approach the critical damping $q = q'\rho^*$ with $q' \ll 1$ [4]. Here, the noise-response overlap (15) spans an intermediate frequency range, in between the characteristic frequencies of the response and the noise $\omega \sim \omega_0^2/\omega_\gamma$, see Fig. 4 (b). Across this range, the integrand in (15) scales as $\omega_\gamma^2/\tau\omega_0^4$, providing the small q scaling $S \sim \omega_\gamma/\tau\omega_0^2$ announced hereinabove (12).

Outlook – Hyperuniformity has been observed across diverse biological systems, from tissues [9–11] to macroecological patterns [12, 13], yet the mechanisms driving its emergence remain unclear. We showed that hyperuniformity naturally arises in a generic class of popula-

tion dynamics models, where death processes are coupled through short-range and indirect interactions between agents. Our formulation is inspired by established mechanisms of cell dynamics in tissues [31], yet the mechanism is general and reflects the sharp increase in agent longevity near a bifurcation. These results open a new avenue for mechanistic investigations into the origins of hyperuniformity in natural systems by identifying its underpinnings in non-conservative population dynamics.

More broadly, our dynamical framework highlights the possibility that many agents can collectively self-tune to critical states by interacting through a spatial field. Our analysis centered on the saddle-node bifurcation, a fundamental transition that captures discontinuous shifts in system dynamics. Other bifurcations have also been explored in biological contexts; for example, critical tuning to a Hopf bifurcation has been implicated in the mechanisms underlying hearing [42]. Extending such frameworks to include spatial dynamics, as we have done here, may reveal new emergent phenomena with potentially important physiological consequences [43].

We thank Ivan Lobaskin, Robert L. Jack, Filippo De Luca and Xiao Ma for useful discussions. B.D.S. and T.A. are supported by the Wellcome Trust (219478/Z/19/Z) and B.D.S. by a Royal Society EP Abraham Research Professorship (RP/R/231004).

-
- [1] Torquato S and Stillinger F H 2003 *Phys. Rev. E* **68** 041113 ISSN 1063-651X, 1095-3787
 - [2] Torquato S 2018 *Physics Reports* **745** 1–95 ISSN 03701573
 - [3] Lei Y and Ni R 2025 *J. Phys.: Condens. Matter* **37** 023004 ISSN 0953-8984, 1361-648X
 - [4] See supplemental Material
 - [5] Donev A, Stillinger F H and Torquato S 2005 *Phys. Rev. Lett.* **95** 090604 ISSN 0031-9007, 1079-7114
 - [6] Tjhung E and Berthier L 2015 *Phys. Rev. Lett.* **114** 148301 ISSN 0031-9007, 1079-7114
 - [7] Weijs J H, Jeanneret R, Dreyfus R and Bartolo D 2015 *Phys. Rev. Lett.* **115** 108301 ISSN 0031-9007, 1079-7114
 - [8] Zhang B and Snezhko A 2022 *Phys. Rev. Lett.* **128** 218002 ISSN 0031-9007, 1079-7114
 - [9] Kram Y A, Mantey S and Corbo J C 2010 *PLoS ONE* **5** e8992 ISSN 1932-6203
 - [10] Jiao Y, Lau T, Hatzikirou H, Meyer-Hermann M, Joseph C Corbo and Torquato S 2014 *Phys. Rev. E* **89** 022721 ISSN 1539-3755, 1550-2376
 - [11] Liu Y, Chen D, Tian J, Xu W and Jiao Y 2024 *Phys. Rev. Lett.* **133** 028401 ISSN 0031-9007, 1079-7114
 - [12] Ge Z 2023 *Proc. Natl. Acad. Sci. U.S.A.* **120** e2306514120 ISSN 0027-8424, 1091-6490
 - [13] Hu W, Liu Q X, Wang B, Xu N, Cui L and Xu C 2023 Disordered hyperuniformity signals functioning and resilience of self-organized vegetation patterns comment: 34 pages, 6 figures; Supplementary Materials, 19 pages, 10 figures, 2 tables (*Preprint* 2311.07624)
 - [14] Florescu M, Torquato S and Steinhardt P J 2009 *Proc.*

- Natl. Acad. Sci. U.S.A.* **106** 20658–20663 ISSN 0027-8424, 1091-6490
- [15] Man W, Florescu M, Williamson E P, He Y, Hashemizad S R, Leung B Y C, Liner D R, Torquato S, Chaikin P M and Steinhardt P J 2013 *Proc. Natl. Acad. Sci. U.S.A.* **110** 15886–15891 ISSN 0027-8424, 1091-6490
- [16] Leseur O, Pierrat R and Carminati R 2016 *Optica* **3** 763 ISSN 2334-2536
- [17] Kim J and Torquato S 2018 *Phys. Rev. B* **97** 054105 ISSN 2469-9950, 2469-9969
- [18] Ma X, Pausch J and Cates M E 2023 Theory of Hyperuniformity at the Absorbing State Transition (*Preprint* 2310.17391)
- [19] Corté L, Gerbode S J, Man W and Pine D J 2009 *Phys. Rev. Lett.* **103** 248301 ISSN 0031-9007, 1079-7114
- [20] Hexner D and Levine D 2017 *Phys. Rev. Lett.* **118** 020601 ISSN 0031-9007, 1079-7114
- [21] Hexner D and Levine D 2015 *Phys. Rev. Lett.* **114** 110602 ISSN 0031-9007, 1079-7114
- [22] De Luca F, Ma X, Nardini C and Cates M E 2024 *J. Phys.: Condens. Matter* **36** 405101 ISSN 0953-8984, 1361-648X
- [23] Lei Q L and Ni R 2019 *Proc. Natl. Acad. Sci. U.S.A.* **116** 22983–22989 ISSN 0027-8424, 1091-6490
- [24] Cengio S D, Mari R and Bertin E 2024 Giant density fluctuations in locally hyperuniform states (*Preprint* 2410.18741)
- [25] Ma X, Pausch J, Pruessner G and Cates M E 2025 Hyperuniformity at the Absorbing State Transition: Perturbative RG for Random Organization comment: This is an expanded and clarified version of arXiv:2310.17391, which it now supersedes without changing the main results (*Preprint* 2507.07793)
- [26] Mukherjee A, Tapader D, Hazra A and Pradhan P 2024 *Phys. Rev. E* **110** 024119 ISSN 2470-0045, 2470-0053
- [27] Hazra A, Mukherjee A and Pradhan P 2025 *J. Stat. Mech.* **2025** 023201 ISSN 1742-5468
- [28] Maire R and Chaix L 2025 Hyperuniformity and conservation laws in non-equilibrium systems comment: 25 pages, 5 figures (*Preprint* 2509.04242)
- [29] Bagci E, Vodovotz Y, Billiar T, Ermentrout G and Bahar I 2006 *Biophysical Journal* **90** 1546–1559 ISSN 00063495
- [30] Tyson J J and Novak B 2014 *Interface Focus*. **4** 20130070 ISSN 2042-8898, 2042-8901
- [31] Simons B D and Karin O 2024 *Immunity* **57** 600–611.e6 ISSN 10747613
- [32] Karin O, Miska E A and Simons B D 2023 *Cell Systems* **14** 24–40.e11 ISSN 24054712
- [33] Simons B D and Karin O 2025 Cell cycle criticality as a mechanism for robust cell population control
- [34] Bak P, Tang C and Wiesenfeld K 1987 *Phys. Rev. Lett.* **59** 381–384 ISSN 0031-9007
- [35] Watkins N W, Pruessner G, Chapman S C, Crosby N B and Jensen H J 2016 *Space Sci Rev* **198** 3–44 ISSN 0038-6308, 1572-9672
- [36] Boxler P 1989 *Probab. Th. Rel. Fields* **83** 509–545 ISSN 0178-8051, 1432-2064
- [37] Hathcock D and Sethna J P 2021 *Phys. Rev. Research* **3** 013156 ISSN 2643-1564
- [38] The normal form (3) has a non-dimensional form for the viability ν and time t , measured with respect to a natural time and viability scale of the individual's internal dynamics. Similarly, the resource c is non-dimensional by virtue of a re-scaled proportionality constant in (4).
- [39] Little J D C 1961 *Operations Research* **9** 383–387 ISSN 0030-364X, 1526-5463
- [40] Nisbet R M and Gurney W S C 2003 *Modelling Fluctuating Populations* (Caldwell, N.J: Blackburn Press) ISBN 978-1-930665-90-3 originally published: New York : Wiley, c1982
- [41] We also set the noise ξ to vanish in the past $t < 0$, to comply with $\delta\rho(t < 0) = 0$
- [42] Camalet S, Duke T, Jülicher F and Prost J 2000 *Proc. Natl. Acad. Sci. U.S.A.* **97** 3183–3188 ISSN 0027-8424, 1091-6490
- [43] Mora T and Bialek W 2011 *J Stat Phys* **144** 268–302 ISSN 0022-4715, 1572-9613